ATLAS Internal Note
TILECAL-NO-039
6 December 1994

The Tilecal laser monitoring

Z. AJALTOUNI, F. BADAUD, N. BOUHEMAID, PH. BRETTE, M. BROSSARD, R. CHADELAS, J.C. CHEVALEYRE, M. CROUAU, F. DAUDON, J.J. DUGNE, F. DURAND[1], C. FAYARD, G. LENTIGNAC, S. MAYADE, B. MICHEL, G. MONTAROU, G.S. MUANZA, J. NIGON[1], D. PALLIN, F. POZZOBON, S. POIROT, E. SAHUC, R. SAIGNE, G. SAVINEL, L.P. SAYS, F. VAZEILLE, D. VINCENT

LPC Clermont-Ferrand
Université Blaise Pascal, IN2P3/CNRS
63177 AUBIERE Cedex France

Abstract

The main goals of the laser monitoring system of the Atlas Hadronic Tile Calorimeter are presented. Then a whole description of the laser monitoring prototype is given. The first test beam results show that the laser intensity is measured at a level of 0.1% Based on these performances, the laser system is expected to continuously monitor the PMTs (and the associated electronics behind) during the Atlas data taking with a precision of 0.5% or better.

[1]COMETT fellow.

This ATLAS note explains the key points of the Tilecal laser monitoring. The main goals are presented in a first part. The part 2 gives the characteristics of the Laser Diode System. The prototype arrangement of the laser monitoring is explained in part 3. Then in part 4 are shown the test beam results, first about the stability of the photodiodes monitoring the laser, and secondly the data of the laser itself. Finally in part 5 are presented the conclusion and the prospects towards the Laser System in the ATLAS framework.

1 ATLAS goals

1.1 Brief description

The calibration, the intercalibration and the monitoring of the ATLAS Hadronic Tile Calorimeter will require several systems based, in particular, on a movable radioactive cesium source [1] and on a laser-driven light pulsing system.

The main purpose of the laser monitoring is to provide a full short time monitoring of the PMTs and their downstream electronics. This monitoring should be obtained with an accuracy of about 0.5% per PMT by using well calibrated laser light pulses.

The core of this system is a frequency-doubled YLF solid-state laser, both externally triggerable and modulated, fully computer controlled. The produced light pulses should have characteristics similar to the light delivered by particles in the calorimeter. The intensity of each pulse is measured by photodiodes used as laser monitors. The absolute stability of the photodiodes and of the associated electronics is controlled using alpha particles from an americium radioactive source. In order to obtain the required accuracy on a large dynamics range, several photodiodes will be used with an overlap of the information. During a bunch-free period, the laser is drived to produce trains of light pulses of increasing intensity, spanning the PMT dynamic range, sent to the calorimeter PMTs and to the laser monitors (photodiodes and a fast PMT for the timing).

1.2 Monitoring goals

The laser system is used to follow continuously the calorimeter PMTs. It plays several rôles:

- a fast on-line control of the working of the PMTs and the associated electronics Frontend,
- a measurement of the time drift of the PMT relative gains,
- a measurement of the linearity of each PMT,
- a measurement of the number of photoelectrons per picocoulomb, which leads to the individual absolute gain of each PMT.

The absolute and time drift gains measurements can be correlated to the radioactive cesium source monitoring.

Could be considered also the possibility to check the level 1 trigger by analyzing sequentially thanks to the Frontend the laser light according to the calorimeter towers.

1.3 Overall performances

The present laser monitoring prototype as described below uses 3 photodiodes (covering the same dynamics for redundancy and a better accuracy) and a train of 16 light pulses is sent to the 200 PMTs of the Tilecal prototype. The laser light has been controlled at a level of 0.1% all along our last test beam period (see part 4). For ATLAS, we could increase the number of pulses to fit the whole dynamics range, without any difficulties.

As an illustration, figures 1-a and 1-b show the 16 laser pulses recorded, respectively, by one photodiode and one Tilecal PMT. The pulses have been adjusted to cover fully the energy dynamic range of pions. Due to both the best quantum efficiency of the photodiodes and the largest amount of the incoming light, the photodiode spectrum 1-a offers a better 'energy' resolution than the PMT spectrum 1-b. We will see in part 2 that, for a given electronic amplitude modulating the laser, there will be pulse-to-pulse laser fluctuations. These fluctuations contribute to enlarge the 16 light pulses. Nevertheless, measuring event by event the light pulses, all the points in figure 1 are individually used to compare the PMTs and the laser (via the 3 photodiodes), which is shown in figure 2.

We can see in figure 10 the alpha spectra taken by the photodiodes. The asymmetry is due to the loss of energy and the energy straggling of alpha particles in the small air gap (of about 1 mm) between the radioactive source and the silicon detectors. These spectra are a direct measurement of the stability of the monitoring of the laser system.

2 Description of the Laser Diode System

2.1 Main components

The Spectra-Physics Laser Diode System [2] is made of two main parts :

- the laser pump : two laser diodes are used and combined in a single beam thanks to a dielectric mirror,
- the laser head : the laser medium and the cavity are coupled to a Q-switch (in order to deliver light pulses) and to a frequency doubler (to generate light outputs in the green region).

2.2 Operation summary [2]

The pump laser diodes excite the Ytrium Lithium Fluoride (Nd:YLF) solid state laser medium, the pump light being delivered to the laser medium through an optical fiber. Two laser diodes are used in order to increase the total power.

These diodes have wavelengths larger than the absorption peak of the laser medium. For maximum efficiency, thermo-electric coolers bring the diodes temperatures down until the output wavelengths match the absorption peak. Tanks to the use of the fiber, no electric energy for diode power or diode cooling is required in the laser head.

The pulse mode operation is given by an acousto-optic Q-switch, acting by an rf signal. With the rf on, no lasing takes place and energy is stored in the laser medium. When the rf is switched off, the laser begins to oscillate. After reaching a maximum, the laser pulse falls as the population inversion is depleted. The process is repeated when the rf is then once again applied.

Attached directly to the Q-switched laser head, a frequency doubler transforms the infra-red light emitted by the laser head (at 1047 nm) in a green light (at 523 nm). This doubler must work in the range 18 to 28°C to be fully efficient.

Extracted from the Spectra-Physics manual, Figure 3 shows the general System Block Diagram.

2.3 Laser characteristics

The laser performances are summarized below:

Output characteristics

Wavelength (nm)	:	523	
Pump power (W)	:	2×1	(maximum value)
Max. energy per pulse (μJ)	:	2×20	(at 800 Hz)
Pulse width (ns)	:	< 15	(at max. energy and 800 Hz)
Beam diameter (mm)	:	0.58	
Beam divergence (mrad)	:	0.7	

Ouput stability (Pulse to pulse)

Energy	rms	:	4%
	3 sigmas	:	±12%

3 Prototype arrangement

A first prototype has been build and tested in 1993. The results validate the approach of using a solid-state laser externally triggerable and modulated, monitored by photodiodes, in order to follow the evolution of the Tilecal PMTs [3].

The prototype described in this ATLAS note corresponds to a second step, with a better survey of the external parameters, the commands fully computer controlled and an improvement of the performances.

3.1 Description

A simplified scheme is shown in figure 4. There are two data acquisition levels: the "General DAQ" (shared with particles and other monitoring elements) and the "Laser VME DAQ" (specific to the laser system). The electronics is located both in the experimental area and in the Tilecal counting room. In a stand-alone working, the calorimeter is supported by a moveable table. The fiber link between the Tilecal and the laser box could be sensitive to the table movements, so attaching the laser box and the fibers to the table prevents any light changes. It will be different in the ATLAS framework (see part 5).

A simplified overview of the laser system is shown in figure 5. The VME system controls :

- the various mechanisms,
- the electronic pulse train generation (16 independent pulses) giving the laser pulses,
- the data recording (laser or source spectra, temperatures inside the laser box, laser working ...).

The laser pump is outside the laser box. The temperatures and intensities of the laser diodes, and the total laser power are shown on the VME display.

In the laser box the following elements are arranged :

- the laser head and the frequency doubler,
- a first shutter called 'main shutter', to stop the laser light just after the head,
- two adjustable polarizers (to select the light range in the calorimeter PMTs),
- a first optical block to split the light to the laser monitors and to the calorimeter, then the other optical blocks associated respectively to the monitors (photodiodes and PMT) and to the five calorimeter modules,
- a second shutter called 'output shutter', to stop if necessary the laser light to the calorimeter,
- the laser monitors:

    * a fast PMT for the timing,
    * three photodiodes (and the associate electronics) to monitor the laser light,
    * an alpha source (moving on a wheel) to monitor the three photodiodes.

- two temperature probes (probe 1 near the laser head, probe 2 near the photodiodes),
- a thermoelectric cooler to adjust the temperature inside the box, from the two temperature probes information. This temperature is chosen in the range 18-28°C for the best working of the doubler. During our test beam period, the temperature was stabilized at 22.0 ± 0.1°C.

- the injection of a nitrogen gas flow (about 50 liters/hour) prevents a possible water condensation due to the cooler. (A thin water layer on the diodes should stop the alphas).

The box opening causes a laser interlock, the output shutter in the closed position, and a stop of PMT and photodiodes power supplies.

3.2 Optical blocks

It would be difficult to send the same laser pulse intensities on every PMT (200 PMTs on the present prototype, about 10000 PMTs in ATLAS). Besides there are other fluctuation sources like the PMT gain adjustments (different PMTs, cell to cell fluctuations ...). It is required only to record all the laser pulses over the dynamic range of every PMT. Nevertheless the light has to be distributed to the monitors and to the PMTs as uniform as possible. That is the rôle of optical blocks at various levels :

- the first optical block distributes the light to the laser monitors and the calorimeter,
- the secondary blocks are:
  - one block associating some clear fibers from the first block to 4 fibers for the 3 photodiodes and the timing PMT,
  - one block connecting the first block to 5 fibers towards the modules,
- the tertiary blocks set on each module and distributing this light to the 40 PMTs of this module. In the bundle making of the WLS fibers, one clear fiber (per bunch) is glued with the WLS fibers associated to a given PMT.

The best output light uniformity is obtained from optical blocks constituted by a diffusor and a squared light mixer, with an air gap of less 1 mm between the clear fibers and the block. The diffusor is made with glass in the laser box, and with tracing paper on the modules.

For a module, light uniformity between the PMTs is achieved within 10%.

3.3 Operation

On the Laser System are implemented three inputs:

- the trigger input called SYNCHRO,
- the ANALOG input which modulates the light intensity,
- the EMISSION input sets on the laser diodes.

The Laser VME system can act at these three levels (see figure 6):

- on the laser pump, by acting on the ANALOG signals (pulse train) and on the EMISSION signal (continue level if ON),
- on the laser head, by acting on the SYNCHRO signal (pulse signal).

A fourth level, called INTERLOCK, is kept for safety either in the case of an accidental opening of the laser box (in the experimental area) or for a manual fast stop thanks to a red switch in the counting room. The logic diagram is organized such a way to save the laser lifetime.

According to the circumstances the laser mode is automatically selected, except the emergency possibility (interlock). In the combined "particles + laser" working (option "auto"), the laser is under the General DAQ control:

- the operator selects only the laser options EXTERNAL, INTERNAL (with respect to the burst) and SPECIAL (laser alone),
- making Start of Run leads automatically to the three successive operations in the laser VME system:

  * pedestal measurements of photodiodes on VME channels,
  * calibration of photodiodes by the alpha source (using the previous pedestal for substraction),
  * then laser working until the End of Run. The laser pulses from calorimeter PMTs and photodiodes are recorded by the General DAQ.
    In addition, the photodiodes data are taken by the laser VME DAQ for monitoring.

The alpha peak positions (corrected from pedestals) are send to three Pattern Units read event by event by the General DAQ. A direct data VME link to the MAIN DAQ is foreseen in 1995.

In the laser VME part, all the spectra are recorded on disk and cartridge and can be printed on the laser printer.

Because of the local calibration of photodiodes, the laser starts only after some bursts. In order to prevent an accumulation on tapes of laser events when the beam is off, the laser stops automatically every time the physical bursts are empty.

In the other VME option called "anti-auto" the laser working is no longer conditionned by the beam bursts. So full freedom is left to provide the laser light to the calorimeter or not thanks to the shutter command (output shutter). The laser VME DAQ system offers four options:

- pedestal,
- source alone,
- laser alone,
- timer mode, in which the operation (source + laser) is several times repeated.

This VME DAQ is stopped using either the STOP order or when an overflow occurs in a bin.

3.4 On-line laser working

On the VME display are shown the photodiodes histograms, the menus and a spy window giving:

- the date and the time,
- the status of shutters (open, closed),
- the acquisition mode (auto, laser, source, ped, timer),
- the temperatures (2 probes) in the laser box, in °C,
- the temperatures and currents of the laser diodes, in °C and mA respectively,
- the laser power, in mW,
- the photodiode alpha peaks in channels.

The General DAQ on-line monitoring gives access to the PMTs and photodiodes, and to the control of the relative linearity of all the PMTs in the running data, which gives immediately the status of the calorimeter.

3.5 Electronics and DAQ

The timing is given by an Hamamatsu R5600 PMT having the 'metal channel dynode structure'. Thanks to the very short rise time of about 0.6 ns, a classical threshold discriminator is well suited to an accurate timing. It is important to notice that this timing is using the laser light output and not the electronic train of pulses which modulate the laser.

The three photodiodes receive information coming from both the laser (optical fibers) and the moving americium source. Three identical circuits have been made. Each circuit has three parts: a photodiode, a preamplifier and an output stage.

The photodiode is a large area PIN silicon photodiode Hamamatsu S2662, with a 7.5×20 mm^2 rectangular active area and a high quantum efficiency at the laser wavelength, and without a front window.

The preamplifier is an integrated circuit E.J&J (HFD1060). The feedback loop has been adjusted to obtain a shape short enough for working with the standard ADC gate as defined for the Tilecal PMTs. A small capacitor (2.7pF) in parallel with the photodiode is used to inject calibrated charges, in order to measure the linearity of the electronics behind the photodiode.

The output stage drives three outputs for 50 ohms cables towards the two ADCs, associated respectively to the DAQ systems (General DAQ, Laser VME DAQ), and the logics associated to the americium source trigger. Each output has a dynamic range of about 400 mV, the alpha source delivering roughly 50 mV.

The logics diagram is not explained there. It makes possible all the operations as described above.

The laser acquisition system, build in VME, plays several roles:

- data acquisition,
- laser control and monitoring,
- americium source command,
- link with the General DAQ.

The signals from the 3 photodiodes are read in a 12 bits charge-integrating ADC (CAEN V265), with a full scale range of 800 pC.

The second card, made at LPC, delivers 16 synchronized pulses the amplitudes of which are programmable by a DAC. The laser pulses intensity is a function of the height of the electronic pulses. Inside this card, are located also the measurements of temperatures inside the laser box and several characteristics of the laser pump (Temperatures and currents of the 2 laser diodes, total laser power).

The third card, also made at LPC, drives the polarizers and the shutters. The americium source step motor rotation is supervised by a dedicated microcontroller (MC68HC711) and two programmable ASICs (XILINX). This card manages also the thermo-cooling system (Peltier elements) of the laser box.

Written in C language, the software manages the human interface, the histograms presenter and the spy window, and the acquisition itself. VME is using OS9 as an operating system.

4 Test beam results

4.1 Accuracy and Stability of measurements

4.1.1 DATA Selection

This study has been performed using a sample of spectra recorded by the photodiodes in the Laser VME System between September 29 and October 12,1994.

Each registred spectrum is written as a binary file containing ADC channels counts. Three types of samples are available : pedestal spectra, alpha particle spectra and laser spectra. In a normal operating procedure, a pedestal run is first recorded, followed by an alpha run and finally a laser run, resulting in 3 files containing the spectrum of each of the 3 photodiodes.

In our analysis we take into account pedestal and alpha spectra recorded consecutively, and containing sufficient statistics (2000 events for pedestals and 3000 for alpha spectra)

Mean values are computed here in the same way as done in the VME software (to check the reliability):

$$M = \frac{\sum_i channel_i * N_i}{\sum_i channel_i}$$

where N_i stands for events in channel i. The mean values for the pedestal spectra are computed using channels 0 to 4095, and the mean values for alpha spectra are computed considering channels 100 to 4095, in order to eliminate the pedestal events taken on 2 photodiodes over 3 for each alpha trigger. Then, the effect of truncation is eliminated by a correction of the form:

$$M_\alpha^{corr} = M_\alpha + int(M_{ped}) - M_{ped}$$

4.1.2 Results

The figure 7 shows the 3 photodiodes pedestal spectra. Pedestal mean values from all selected files have been calculated and the fits of the resulting distributions (figure 8) give (in ADC channels) :

$$\begin{array}{ll} M_{pied}^{diode1} = 50.98 & \sigma_{pied}^{diode1} \simeq 0.14 \\ M_{pied}^{diode2} = 16.75 & \sigma_{pied}^{diode2} \simeq 0.13 \\ M_{pied}^{diode3} = 38.22 & \sigma_{pied}^{diode3} \simeq 0.09 \end{array}$$

σ's of the distributions illustrate the very small fluctuation of pedestals values. In figure 9 a coherent noise is clearly seen between the photodiodes 1 and 2, that we attribute to a physical noisy correlation in the ADC.

Figure 10 shows the alpha spectra recorded by the 3 photodiodes summed over all the selected files. The distribution of the mean values of the alpha peak (figure 11) gives the following results (in ADC channels) :

$$\begin{array}{ll} M_\alpha^{diode1} = 233.9 & \sigma_\alpha^{diode1} = 0.367 \\ M_\alpha^{diode2} = 229.4 & \sigma_\alpha^{diode2} = 0.358 \\ M_\alpha^{diode3} = 228.1 & \sigma_\alpha^{diode3} = 0.421 \end{array}$$

The fluctuation (less than 2 per mill) is a convolution of the temporal fluctuation and of the precision of the peak value estimation.

The variation in function of the time of the 3 alpha peaks is shown in figure 12. A polynomial fit indicates that this variation is of the order of 0.04% per day. Correcting our measurements for this observed temporal fluctuation allows to estimate with which precision we can define the alpha peak position (i.e. measurement accuracy + choice of the mean value as an estimate of the absolute alpha peak position). This precision is found to be 0.15 %.

According to the previous results, the 3 photodiodes are correctly and similarly working. So, the best estimate of the alpha peak is obtained by combining the 3 photodiodes measurements. One defines, for each alpha run, a unique value of the form :

$$M_\alpha = 1/3 * (M_\alpha^{diode1} + M_\alpha^{diode2} + M_\alpha^{diode3})$$

The distribution of M_α and its dependence in function of the time are shown in figures 13 and 14, resulting in a temporal fluctuation of the order of 0.02% per day with a precision on M_α measurement of 0.095%.

4.1.3 Conclusion

- The VME software will be modified in order to substract a more precise value of the pedestals. The effect of truncation, uncorrectable on the data recorded by the General DAQ program, is of the order of 0.5%
- The accuracy on <u>one</u> alpha peak measurement is of the order of **<u>0.1%</u>**
- The unstability of the alpha peak measurement is of the order of **1/2 channel for 14 days**.
- Thanks to the temperature stabilization inside the laser box, the electronics working stays stable. So, the alpha peak correction should be used only in the case of a sizeable drift.

4.2 Laser Data analysis

As already said in part 1, the Laser System allows to follow the response drift of all PMTs (on-line and off-line), to measure their non linearity, and to determine the number of photoelectrons in function of the charge delivered by the PMTs. These three fields have been explored.

4.2.1 Drift response of the PMTs

The ratio between a PMT response and the average photodiode response gives a relative gain. This has been made first on-line and has given a view of the whole calorimeter stability, and also an immediate detection of individual PMT problems (e.g. a HV fall on 16 channels).

In figure 15, an example of the on-line monitoring is shown. During a special laser run, the ratio PMT/Laser has been measured for every PMT, and registered in the monitoring data bank. These same ratios are continuously calculated during the general data taking, and normalized respectively to the corresponding PMT reference ratios. Fluctuations give access to the PMT gain changes, coming from various sources (the intrinsic PMT stability, the HV drifts, the temperature variations, ...). In figure 15, the status at the end of the test beam period is displayed for the 200 PMTs, with 40 PMTs per module. The last histogram merges the 200 normalized ratios. It appears clearly that the mean drift is at a level of 1%, whereas some PMTs had fluctuations of about 10%, which are under control.

A preliminary off-line analysis of these relative gains confirmed that the calorimeter was stable at a level of 1%.

Figure 16 shows the evolution of the ratio PMT/Laser for a given PMT over a 10 day period. Some fluctuations appear within an interval of $\pm 1.0\%$.

The agreement with the cesium source calibrations is satisfactory and a sharper comparison between the two methods is now in course. This relative gain can be used for particle analysis to renormalize the PMT response in function of the run numbers.

4.2.2 Non linearity of the PMTs

The relative gain of a PMT should change with the output charge. It is why, instead of a single peak, we send trains of 16 laser pulses of different intensities, covering the dynamics of the physics events of the Tilecal prototype. In these conditions, the typical non linearities of PMTs are weak, which is shown for a given PMT in figure 17. It could be different in the ATLAS framework (higher dynamics) and the data could be corrected.

4.2.3 Number of photoelectrons

Statistical considerations give the well known relation $\frac{\sigma}{E} = \frac{1}{\sqrt{N}}$, where E is the charge delivered by a PMT, σ the standard deviation on E, and N the number of photoelectrons incoming from the photocathode. It is easy to see than $\frac{E}{Ne}$ is the absolute gain of the PMT (e is the electron charge). This determination can be a redundancy of the measurement of the relative gain, but less accurate for a given number of events. On an other hand, assuming the cells of the calorimeter are well intercalibrated by the cesium source and calibrated with particles, the number of photoelectrons we measure is proportional to the number of photoelectrons per GeV of the whole cell.

Figure 18 gives an estimate of the number of photoelectrons per pC for three modules. It appears that the module # 3 offers, in average, two times more photoelectrons than the adjacent modules, that is confirmed by other measurements and corresponds to the last optimization of tiles and WLS fibers. Inside a module, the fluctuations correspond to the various PMT gains adjustments.

4.2.4 Conclusion

The laser system is a powerful test and calibration tool. It allows to check very quickly whether the PMTs of the whole calorimeter are running, to measure the drift, the non linearities and the absolute gain of these PMTs and to determine (with the cesium source) the yield of each cell of the calorimeter.

5 Conclusion and future work

This Laser Monitoring System satisfies to the ATLAS Tilecal requirements. Fully computer controlled, this prototype is integrated in the ATLAS test beam area, and connected to the General DAQ.

The laser pulse intensity is controlled at a level of 0.1% and the various objectives relative to the Tilecal PMTs have been tested : the gain drift time measurements, the control of the non-linearities, an approach of the absolute gain from the estimate of the number of photoelectrons per pC.

New upgrades will be done in 1995. First the possibility to inject calibrated charges in order to measure in the experimental conditions the linearity of the photodiode electronics. For safety an additional (independent from VME) cooling will be implemented. In the ATLAS Slow Control context the Laser Monitoring will be tested.

An important goal is to match more closely the two monitoring approaches : the cesium source calibration and the Laser.

Towards the final system for ATLAS, many things should be studied. An increase of the light dynamics could be obtained by an upgrade of the laser, in collaboration with the manufacturer. This possible improvement could be combined from the use of a small number of optical attenuators (2 or 3). But in any cases we will keep the original concept of a triggerable and modulated laser. In the test beam, the polarizers attenuate the laser light by three orders of magnitude. In ATLAS, taking into account the number of PMTs and the biggest incoming energies increase the light intensity by factors close to 50 and 10, respectively. This global gain of about 500 is lower than the present attenuation: thus, this laser is strong enough to be used in ATLAS.

In order to control this biggest dynamics, we have to optimize the number of photodiodes. Other photodiodes could be introduced to measure the ageing of the clear fibers tansporting the laser light to the PMTs, by using similar fibers going towards the Calorimeter and going back without other links. Considering three fibers for the Barrel , and the same for the External Barrels, and doubling the silicon detectors to monitor the laser, we would have finally 15 photodiodes in the laser box to survey.

We have also to find the best arrangement of the Laser System in the ATLAS pit. The Laser Box could be located in the counting room, in order to guarantee a free access. A quartz fiber bundle could transport the laser light all along the 80 meters leading to the ATLAS cavern, without a significative light loss. A patchpanel would distribute the light to the Tilecal modules. Plastic fibers would be used only inside each module, because of the glueing with the WLS fibers. So using in a large part quartz fibers could decrease strongly the radiation damages.

The total number of quartz fibers would be small: for example, 274 = Barrel (2×64 + 2 External Barrels (64) + testing fibers (2×9). Therefore, in the cavern the Laser Monitoring System will need only passive materiel (fibers and connectors).

Obviously many questions are yet open. However, this global approach should be very reliable, in the same spirit as for our choice of the Laser Diode System which offers many advantages over the usual solutions: a longer lifetime, a more compact size, no water cooling and no thermal lensing in the active medium.

References

[1] G. Blanchot et al., ATLAS Internal Note TILECAL-NO-44 (1994)

[2] SPECTRA-PHYSICS, Laser Diode Systems 1250 Charleston Road, Mountain View, CA 94043, USA

[3] F. Ariztizabal et al., Nucl. Instrum. Methods A349 (1994) 384

Figure caption

FIGURE 1: a) and b) - Train of 16 laser light pulses recorded respectively by a photodiode and a Tilecal PMT.

FIGURE 2: Laser response event by event of a Tilecal PMT in function of the photodiode # 1.

FIGURE 3: Block diagram showing the Spectra-Physics Laser Diode System.

FIGURE 4: Simplified scheme showing the two data acquisition levels: General DAQ and Laser VME DAQ.

FIGURE 5: Laser box scheme and Laser VME System.

FIGURE 6: Signals acting the Laser.

FIGURE 7: Pedestals of the three photodiodes.

FIGURE 8: Fits of the photodiode pedestals.

FIGURE 9: Correlation of pedestals of photodiodes 1 and 2.

FIGURE 10: Alpha spectra recorded by the three photodiodes.

FIGURE 11: Distributions of the three mean alpha peaks over the test beam period.

FIGURE 12: Evolutions of the three mean alpha peaks in function of the time, and comparison to polynomial fits.

FIGURE 13: Distribution of the average of the three mean alpha peaks over the test beam period.

FIGURE 14: Evolution of the average of the three mean alpha peaks in function of the time, and comparison to a polynomial fit.

FIGURE 15: On-line monitoring of the 200 Tilecal PMTs: values of the ratio PMT/Laser normalized to the same ratio before taking the first data, at the end of the test beam period: for every 5 modules, and merged in a single histogram.

FIGURE 16: Evolution of the ratio PMT/laser for a given Tilecal PMT in function of the time.

FIGURE 17: Linearity of a given Tilecal PMT, using the laser as a reference.

FIGURE 18: Estimation of the number of photoelectrons/pC for some PMTs in Tilecal modules 2, 3 and 4.

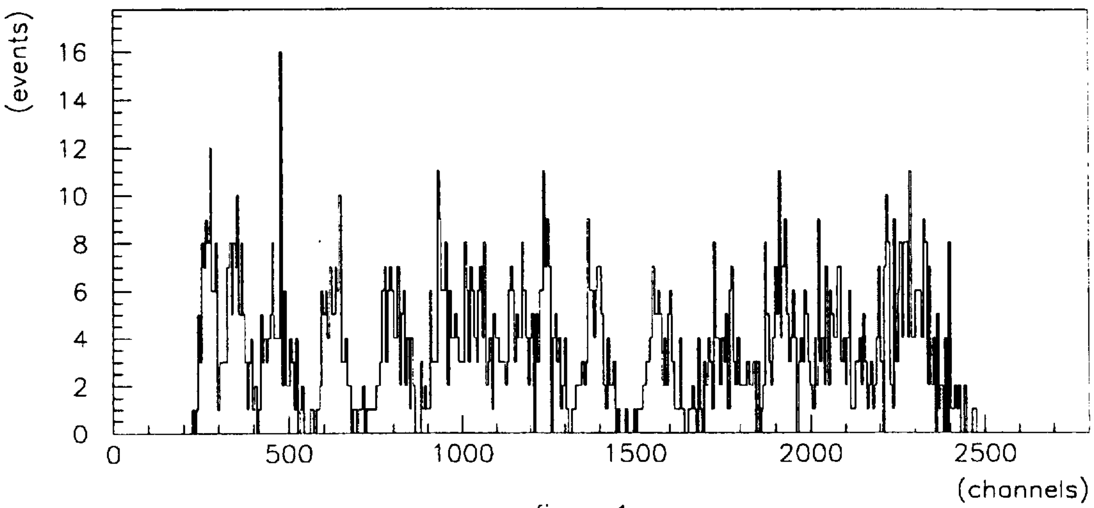

figure 1-a

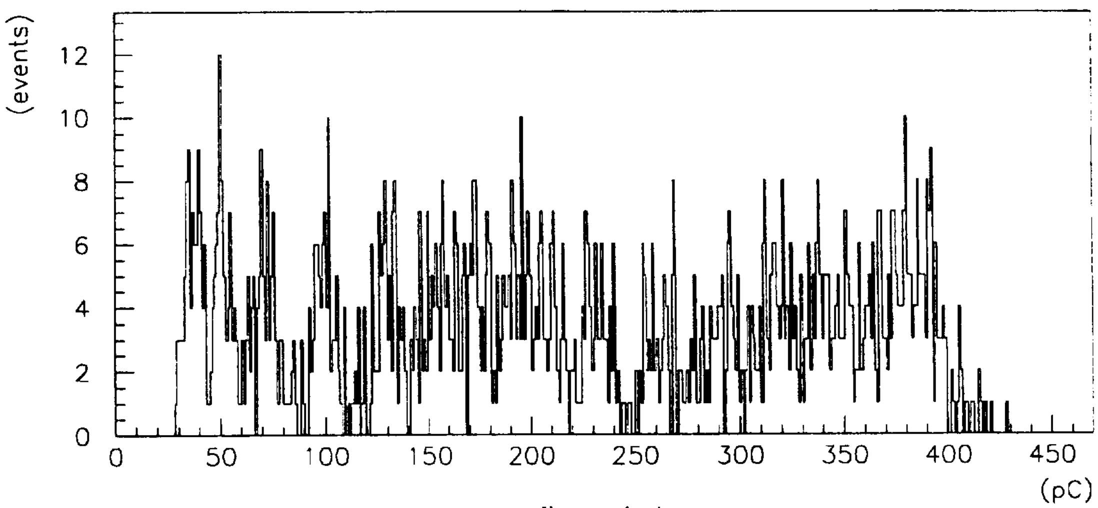

figure 1-b

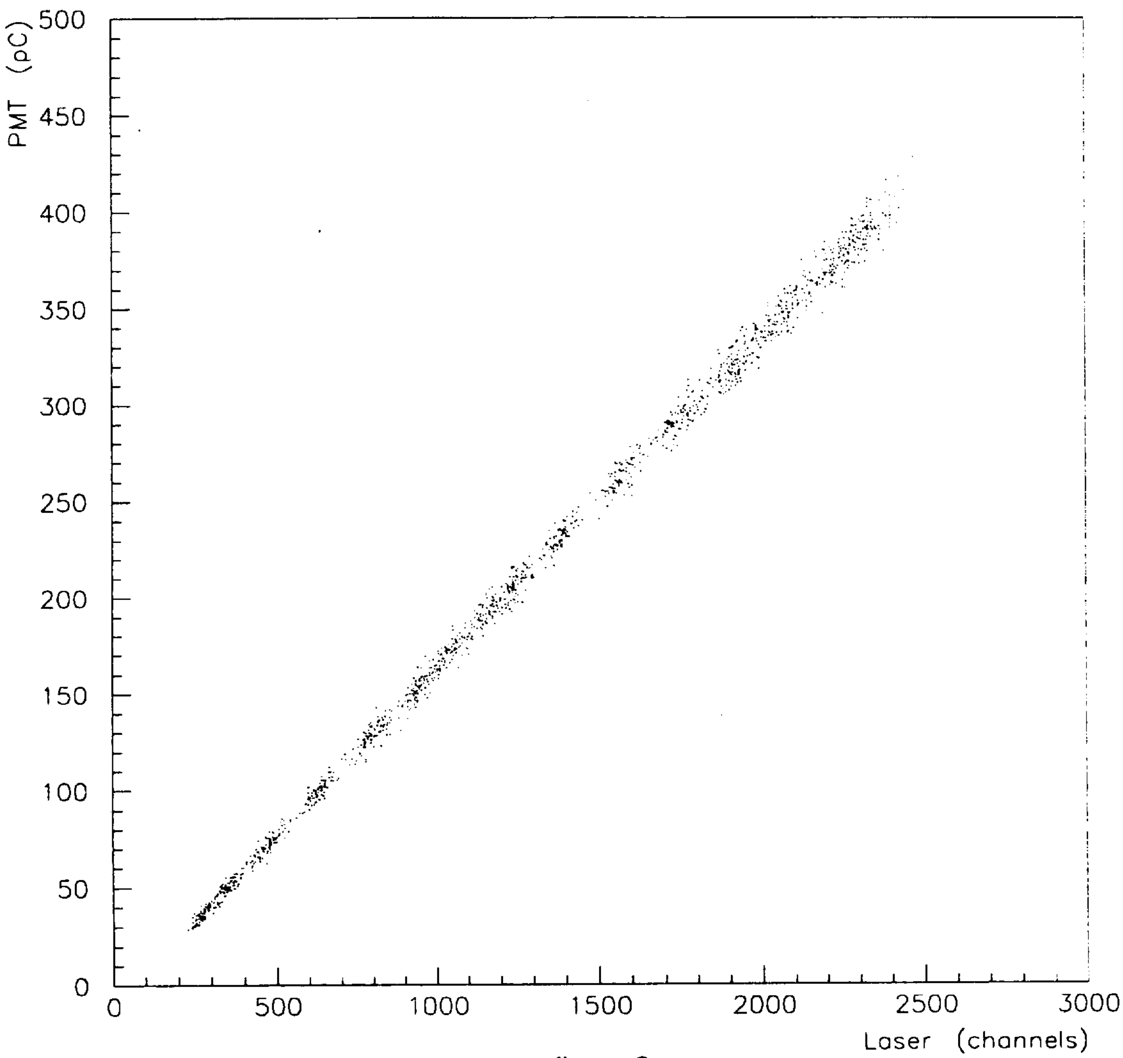
PMT (pC)
500
450
400
350
300
250
200
150
100
50
0
0
500
1000
1500
2000
2500
3000
Laser (channels)

figure 2

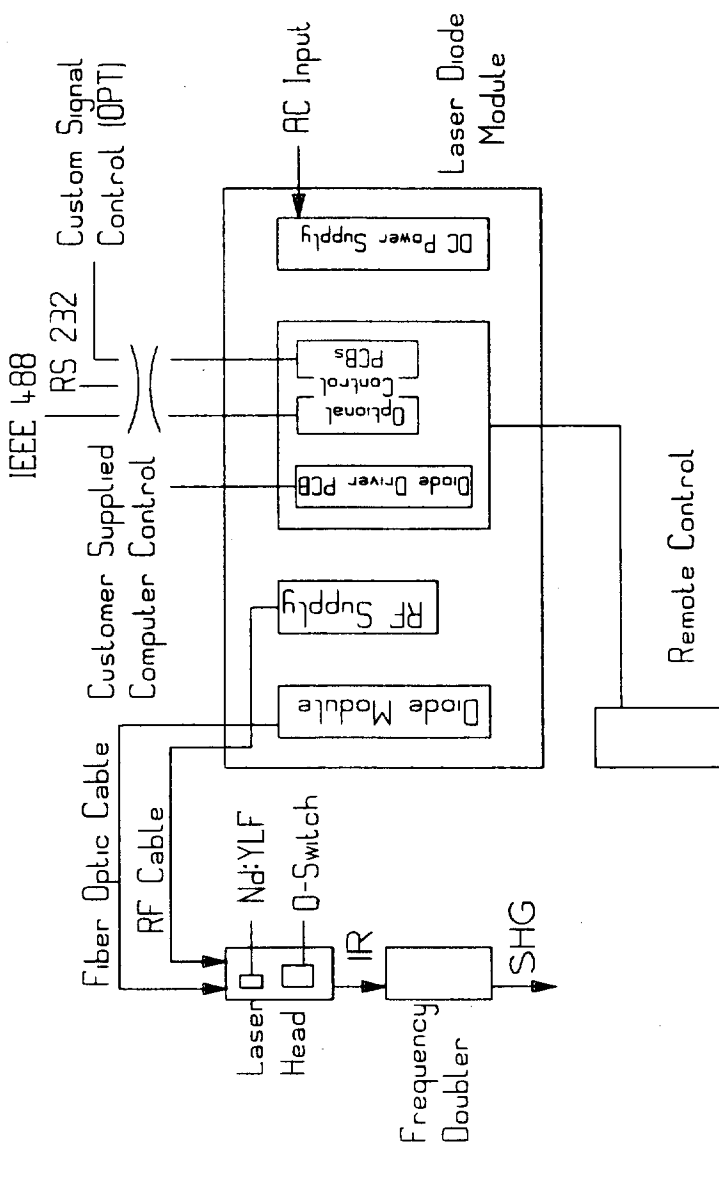
IEEE 488
RS 232
Custom Signal
Control (OPT)
AC Input
Laser Diode
Module
DC Power Supply
Optional
Control
PCBs
Diode Driver PCB
RF Supply
Diode Module
Customer Supplied
Computer Control
Remote Control
Fiber Optic Cable
RF Cable
Nd:YLF
Q-Switch
IR
SHG
Laser
Head
Frequency
Doubler

Figure 3

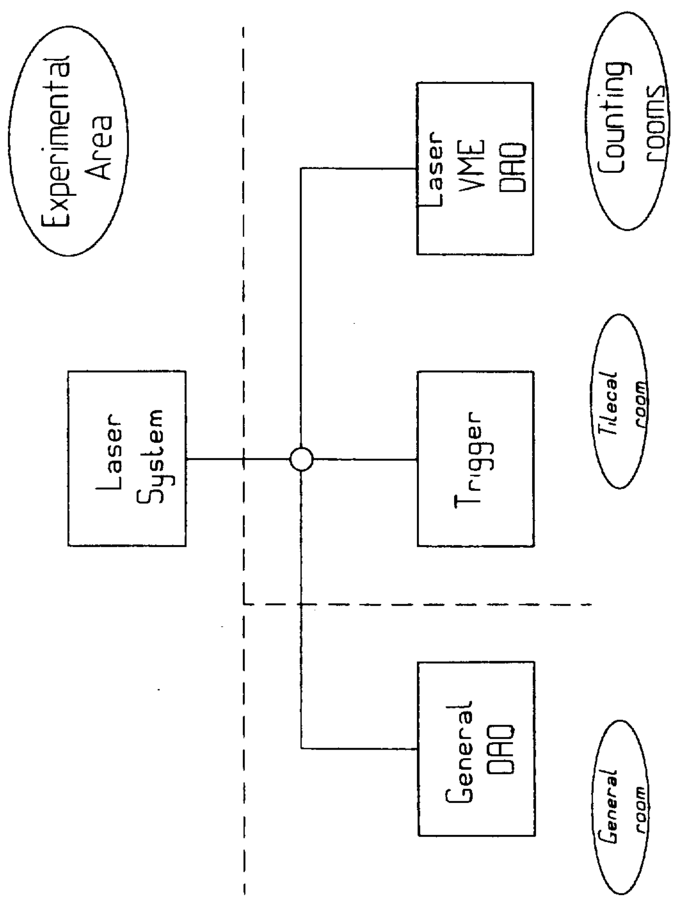
Experimental Area
Laser System
Trigger
Laser VME DAQ
General DAQ
Counting rooms
Tilecal room
General room

Figure 4

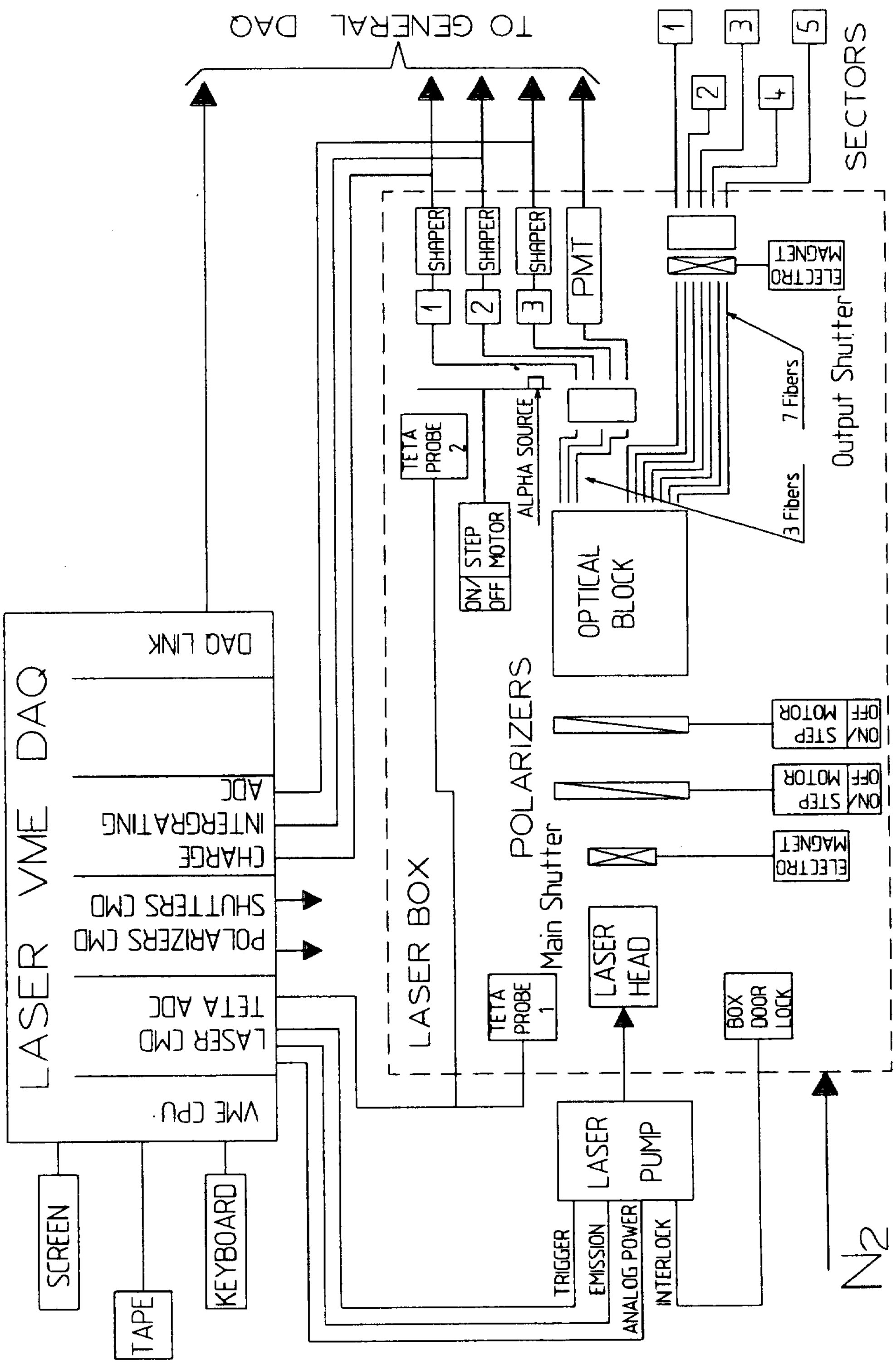
LASER VME DAQ
VME CPU
LASER CMD
TETA ADC
POLARIZERS CMD
SHUTTERS CMD
CHARGE
INTERGRATING
ADC
DAQ LINK
SCREEN
TAPE
KEYBOARD
TO GENERAL DAQ
LASER BOX
TETA PROBE 1
TETA PROBE 2
LASER HEAD
Main Shutter
LASER PUMP
TRIGGER
EMISSION
ANALOG POWER
INTERLOCK
BOX DOOR LOCK
ELECTRO MAGNET
POLARIZERS
ON/OFF STEP MOTOR
OPTICAL BLOCK
ALPHA SOURCE
SHAPER
PMT
3 Fibers
7 Fibers
Output Shutter
SECTORS
N_2

Figure 5

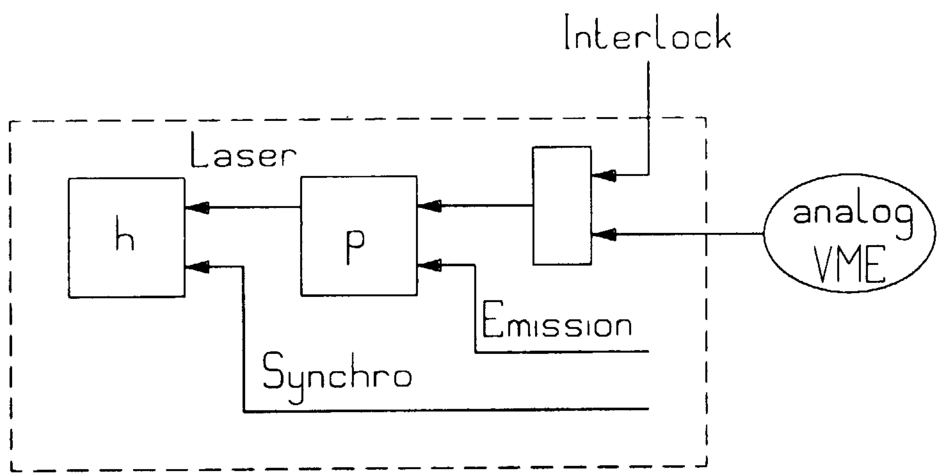

Figure 6

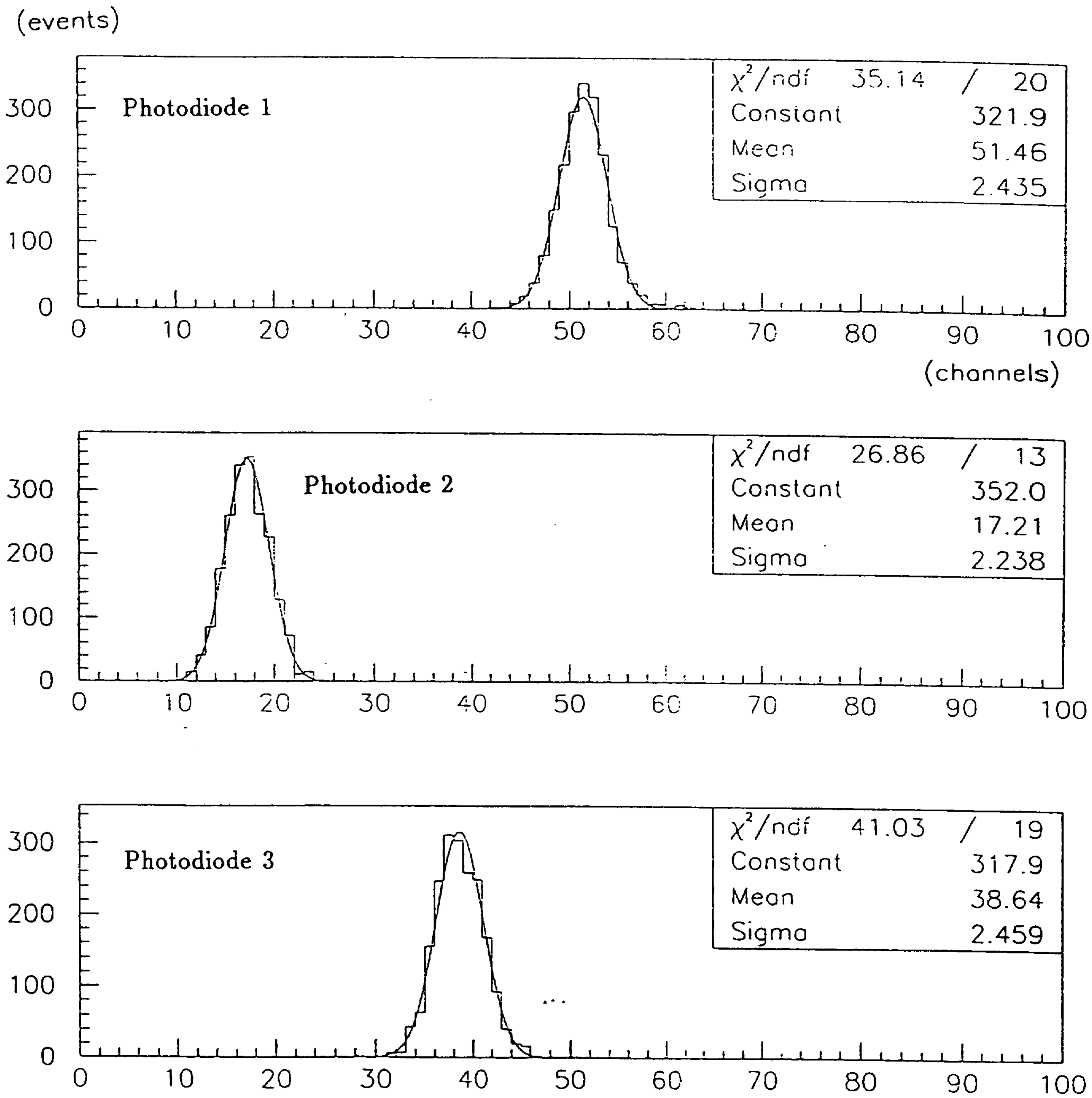
(events)
Photodiode 1
χ^2/ndf 35.14 / 20
Constant 321.9
Mean 51.46
Sigma 2.435
300
200
100
0
0 10 20 30 40 50 60 70 80 90 100
(channels)
Photodiode 2
χ^2/ndf 26.86 / 13
Constant 352.0
Mean 17.21
Sigma 2.238
Photodiode 3
χ^2/ndf 41.03 / 19
Constant 317.9
Mean 38.64
Sigma 2.459

Figure 7

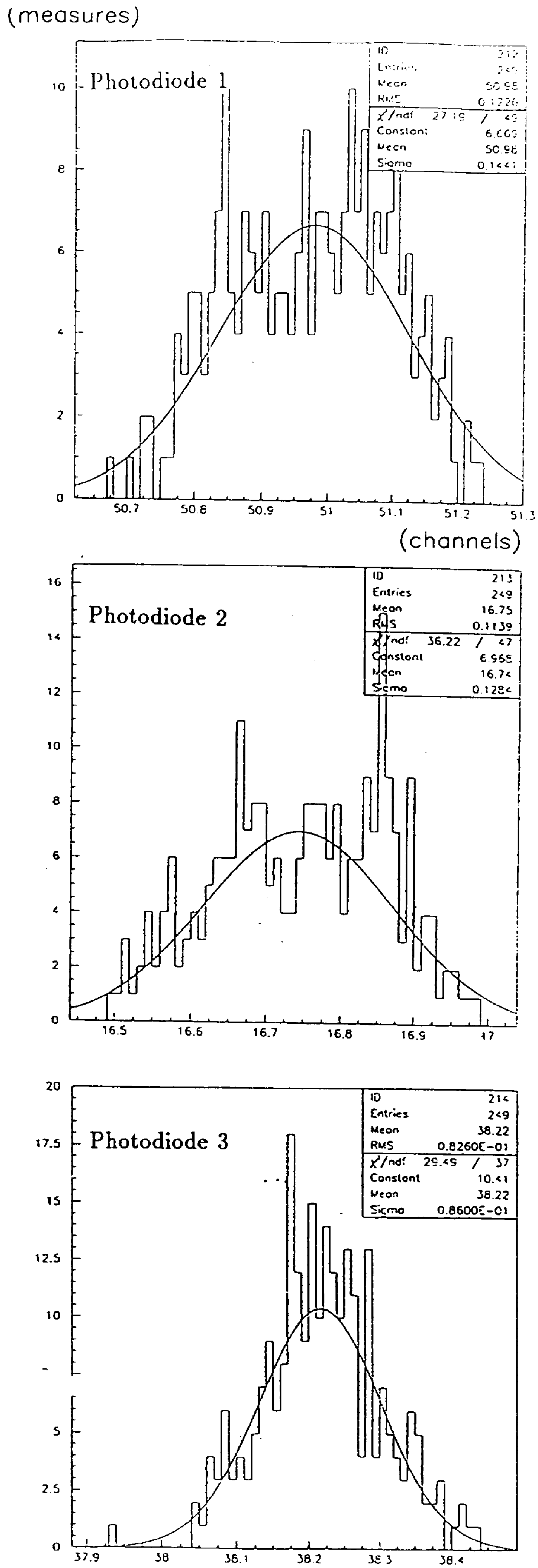
(measures)
Photodiode 1
Mean 50.98
Mean 50.98
(channels)
Photodiode 2
ID 213
Entries 249
Mean 16.75
RMS 0.1139
χ²/ndf 36.22 / 47
Constant 6.965
Mean 16.74
Sigma 0.1284
Photodiode 3
ID 214
Entries 249
Mean 38.22
RMS 0.8260E-01
χ²/ndf 29.49 / 37
Constant 10.41
Mean 38.22
Sigma 0.8600E-01

Figure 8

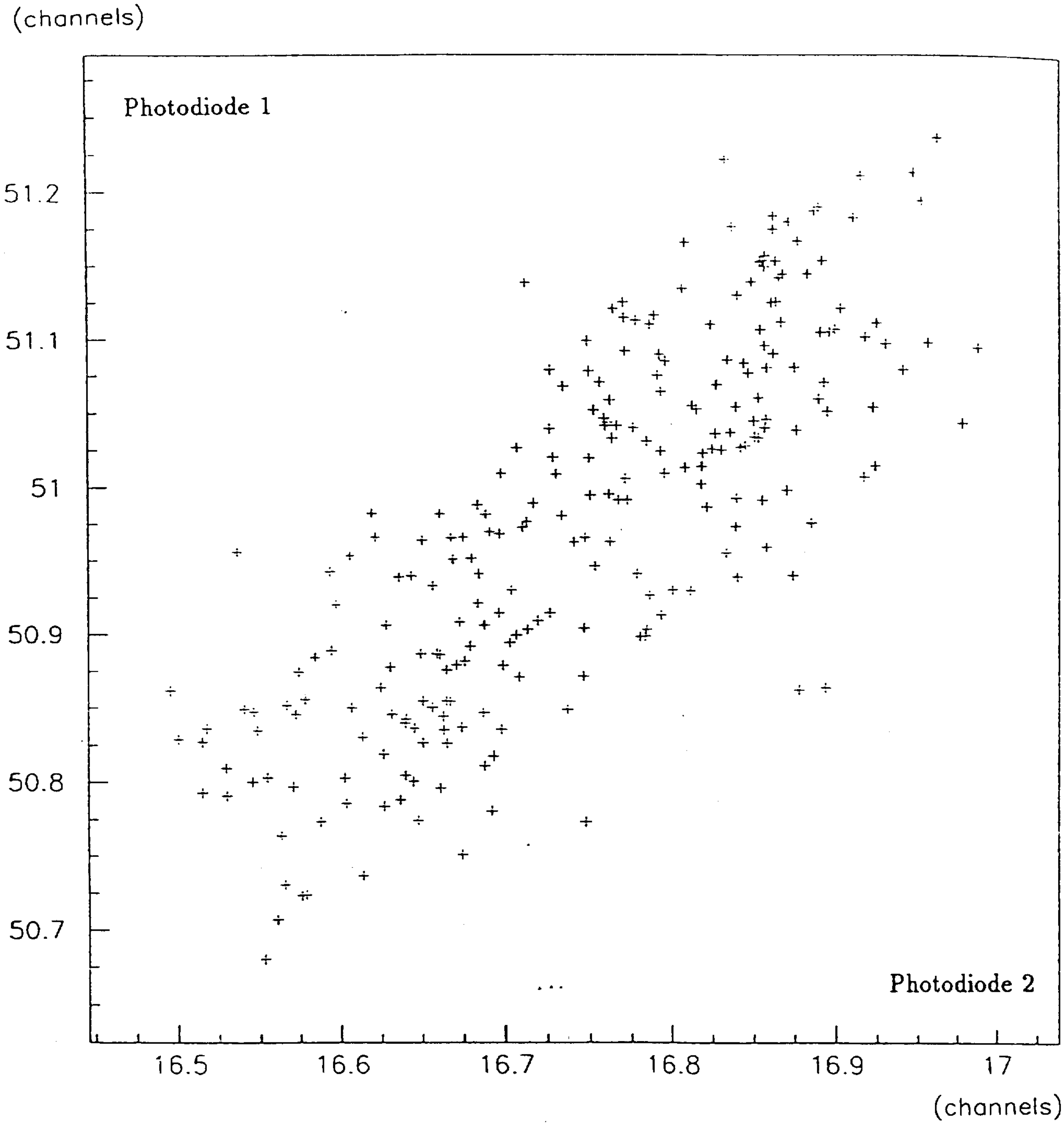
(channels)
Photodiode 1
51.2
51.1
51
50.9
50.8
50.7
Photodiode 2
16.5
16.6
16.7
16.8
16.9
17
(channels)

Figure 9

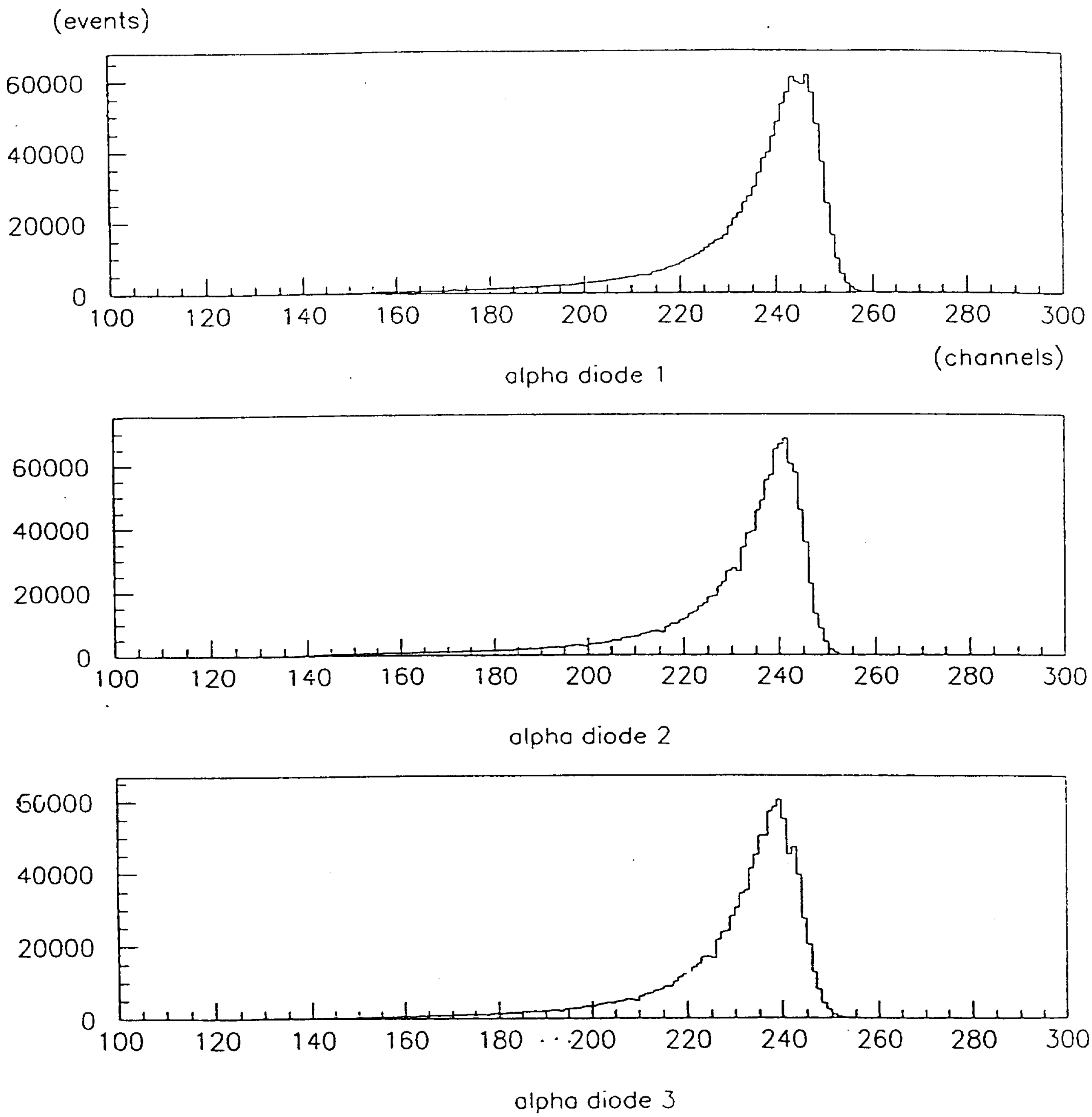
(events)
60000
40000
20000
0
100
120
140
160
180
200
220
240
260
280
300
(channels)
alpha diode 1
60000
40000
20000
0
100
120
140
160
180
200
220
240
260
280
300
alpha diode 2
60000
40000
20000
0
100
120
140
160
180
200
220
240
260
280
300
alpha diode 3

Figure 10

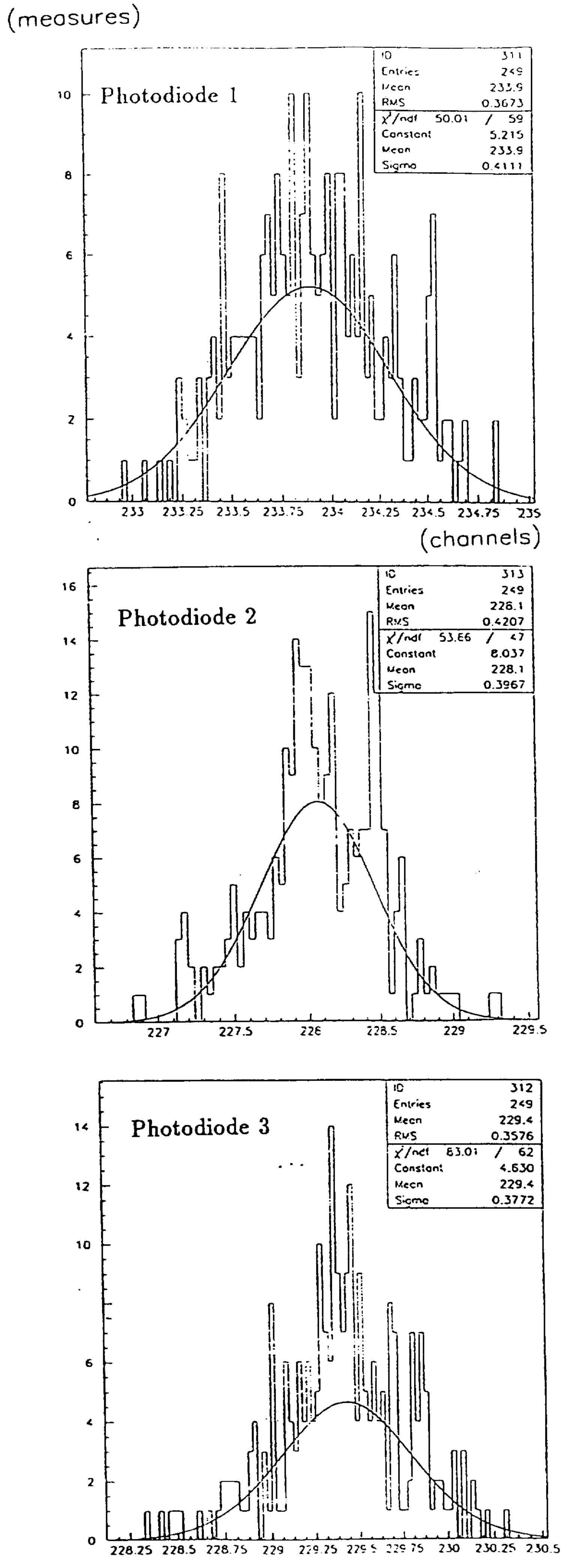
(measures)
Photodiode 1
ID 311
Entries 249
Mean 233.9
RMS 0.3673
χ²/ndf 50.01 / 59
Constant 5.215
Mean 233.9
Sigma 0.4111
(channels)
Photodiode 2
ID 313
Entries 249
Mean 228.1
RMS 0.4207
χ²/ndf 53.66 / 47
Constant 8.037
Mean 228.1
Sigma 0.3967
Photodiode 3
ID 312
Entries 249
Mean 229.4
RMS 0.3576
χ²/ndf 83.01 / 62
Constant 4.630
Mean 229.4
Sigma 0.3772

Figure 11

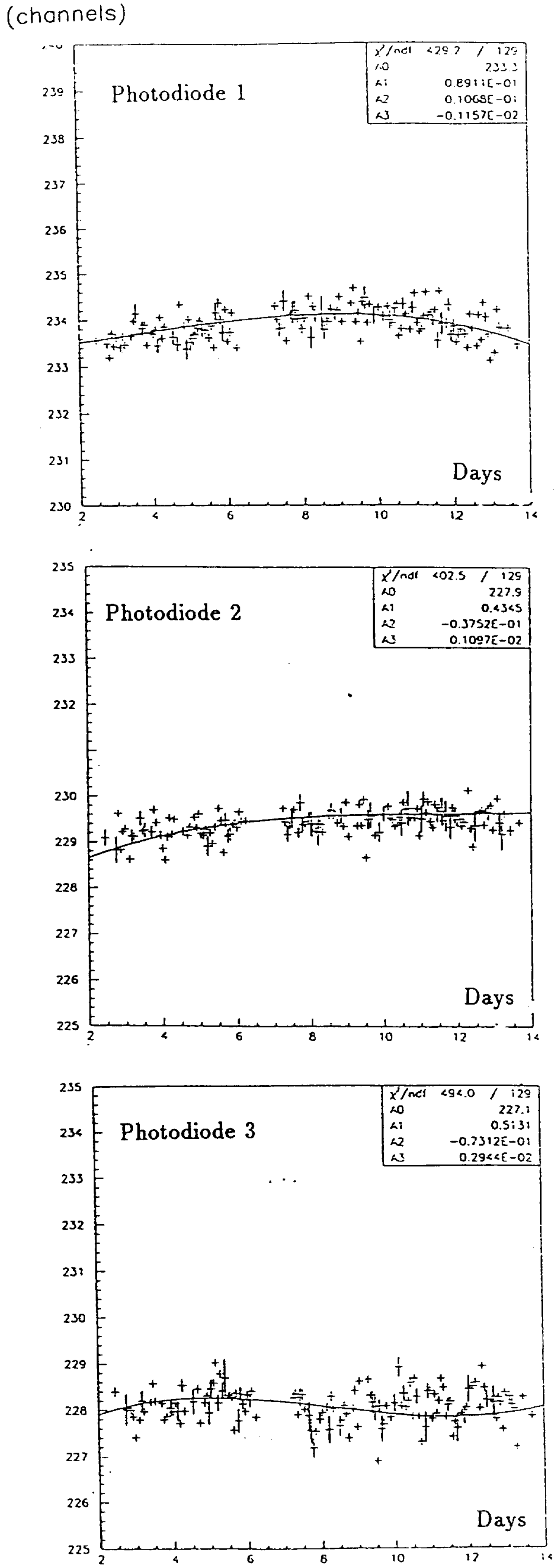
(channels)
Photodiode 1
Days
Photodiode 2
χ²/ndf 402.5 / 129
A0 227.9
A1 0.4345
A2 -0.3752E-01
A3 0.1097E-02
Days
Photodiode 3
χ²/ndf 494.0 / 129
A0 227.1
A2 -0.7312E-01
Days

Figure 12

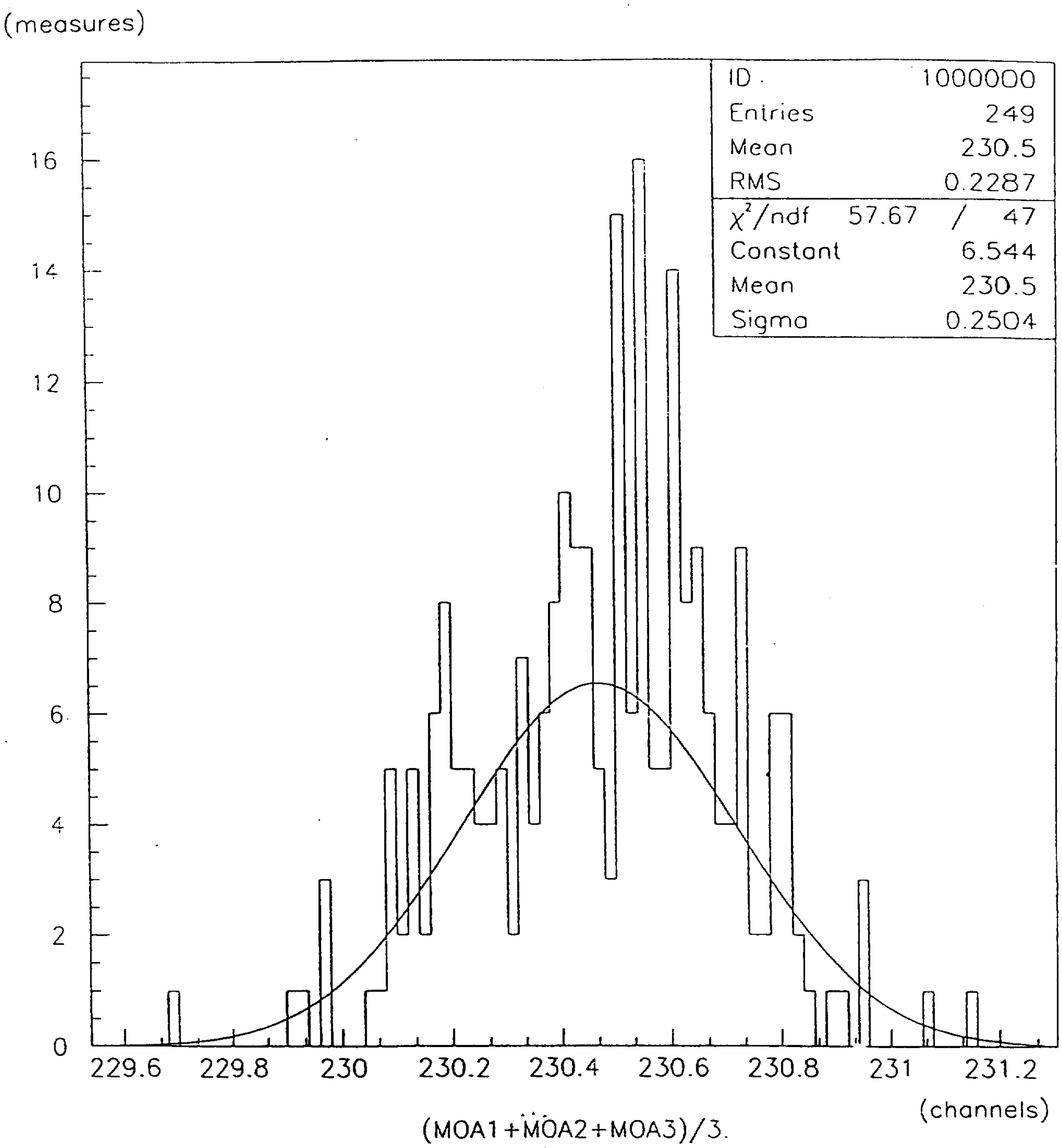
(measures)
ID 1000000
Entries 249
Mean 230.5
RMS 0.2287
χ²/ndf 57.67 / 47
Constant 6.544
Mean 230.5
Sigma 0.2504
16
14
12
10
8
6
4
2
0
229.6
229.8
230
230.2
230.4
230.6
230.8
231
231.2
(channels)
(MOA1+MOA2+MOA3)/3.

Figure 13

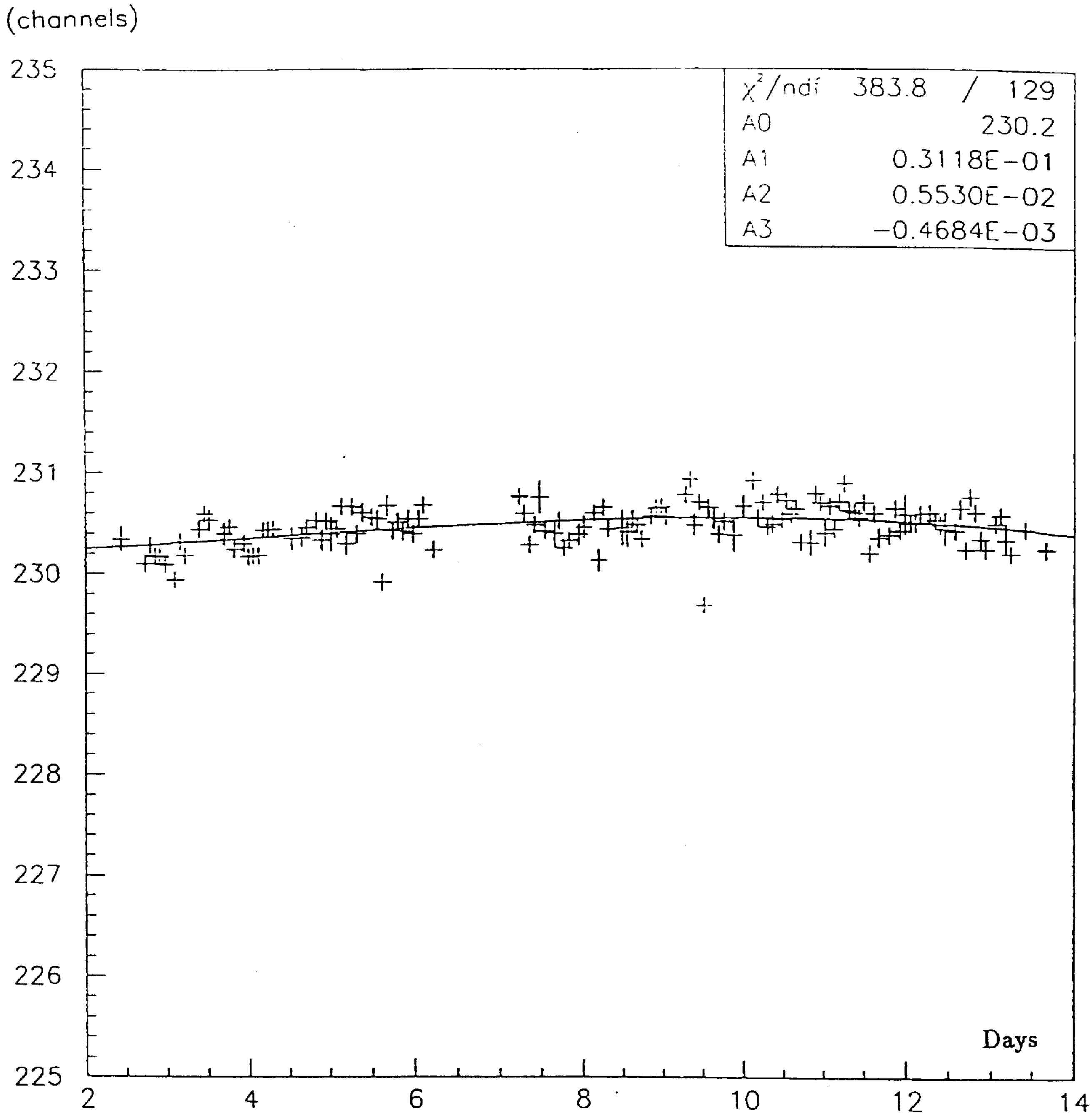
(channels)
235
234
233
232
231
230
229
228
227
226
225
χ^2/ndf 383.8 / 129
A0 230.2
A1 0.3118E-01
A2 0.5530E-02
A3 -0.4684E-03
Days
2
4
6
8
10
12
14

Figure 14

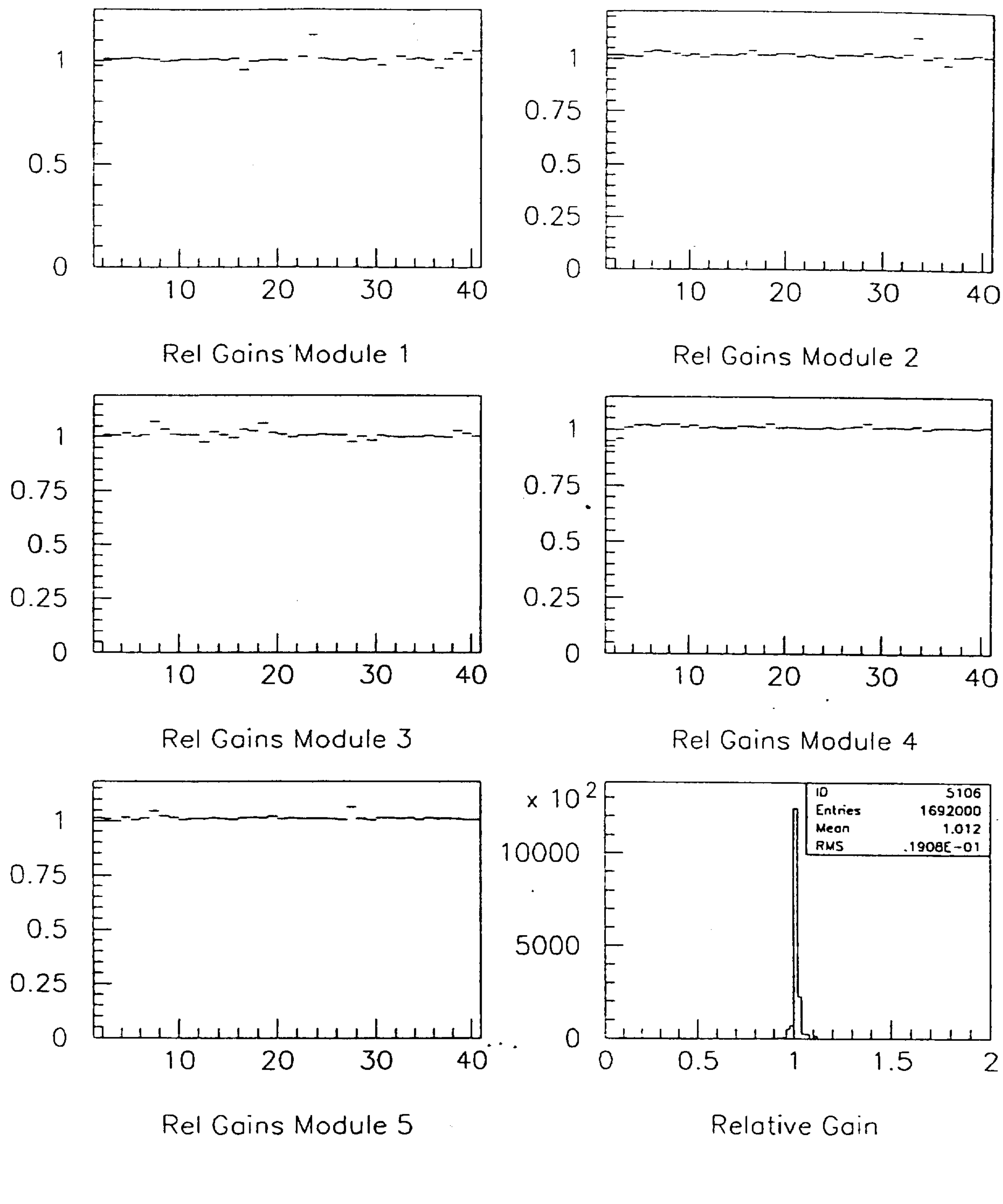

Rel Gains Module 1
Rel Gains Module 2
Rel Gains Module 3
Rel Gains Module 4
Rel Gains Module 5
Relative Gain
x 10^2
ID 5106
Entries 1692000
Mean 1.012
RMS .1908E-01

Figure 15

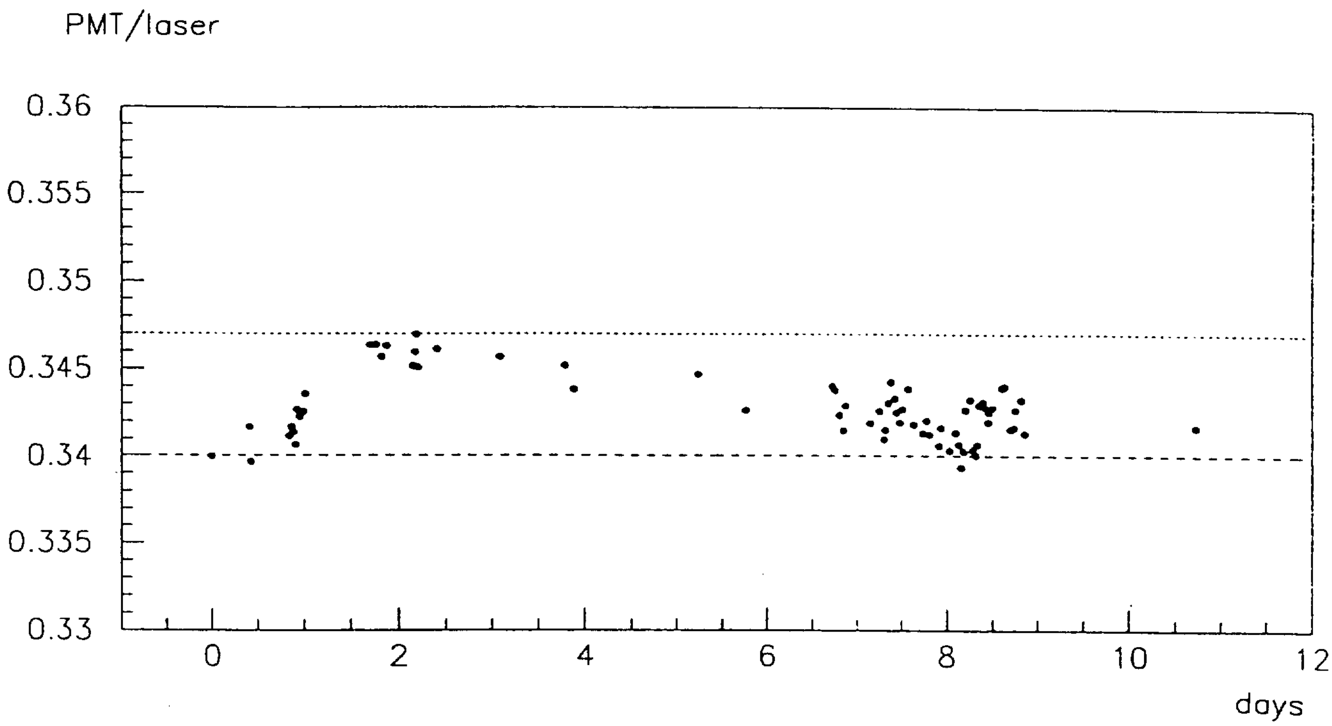

Figure 16

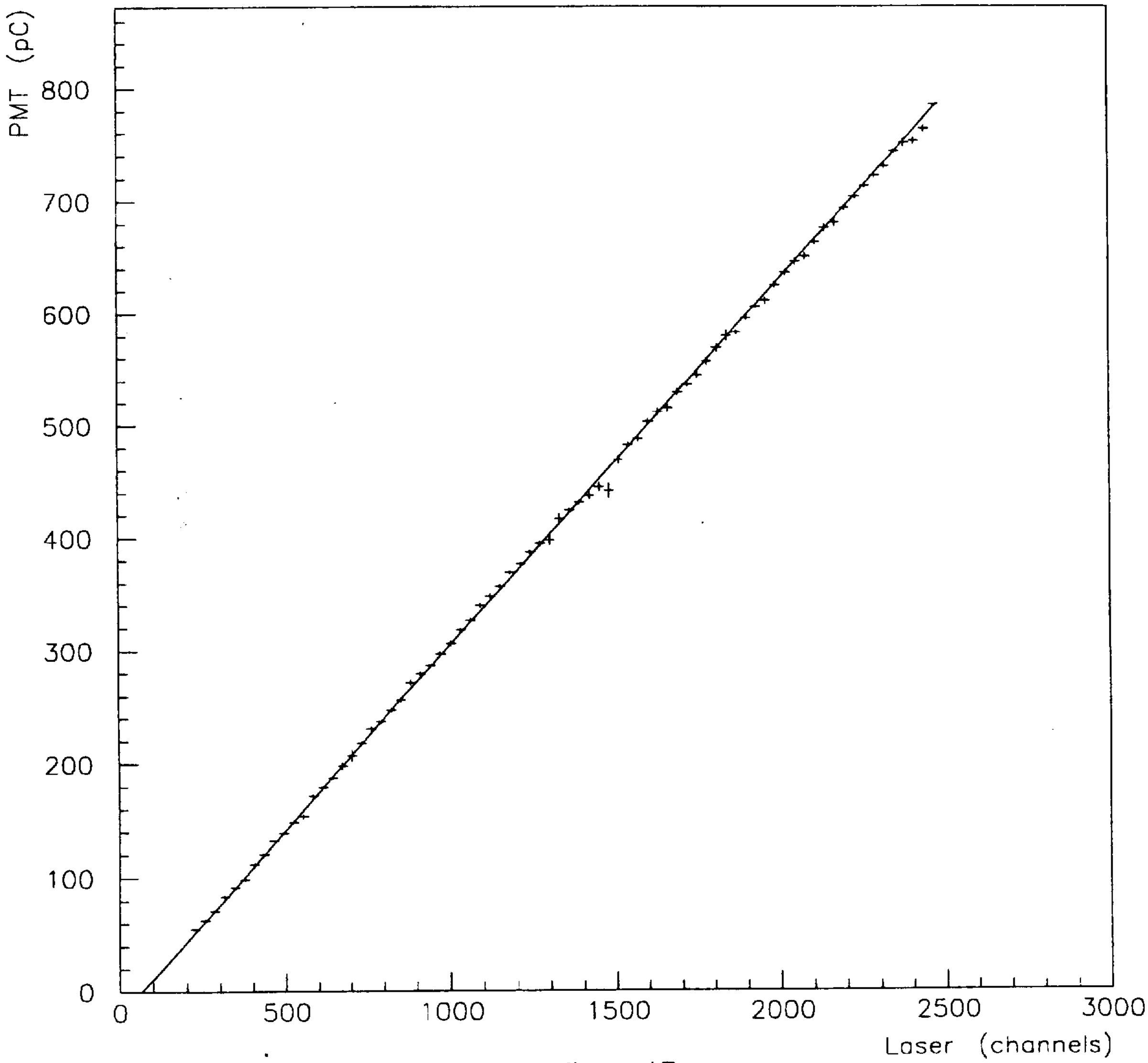
PMT (pC)
800
700
600
500
400
300
200
100
0
0
500
1000
1500
2000
2500
3000
Laser (channels)
figure 17

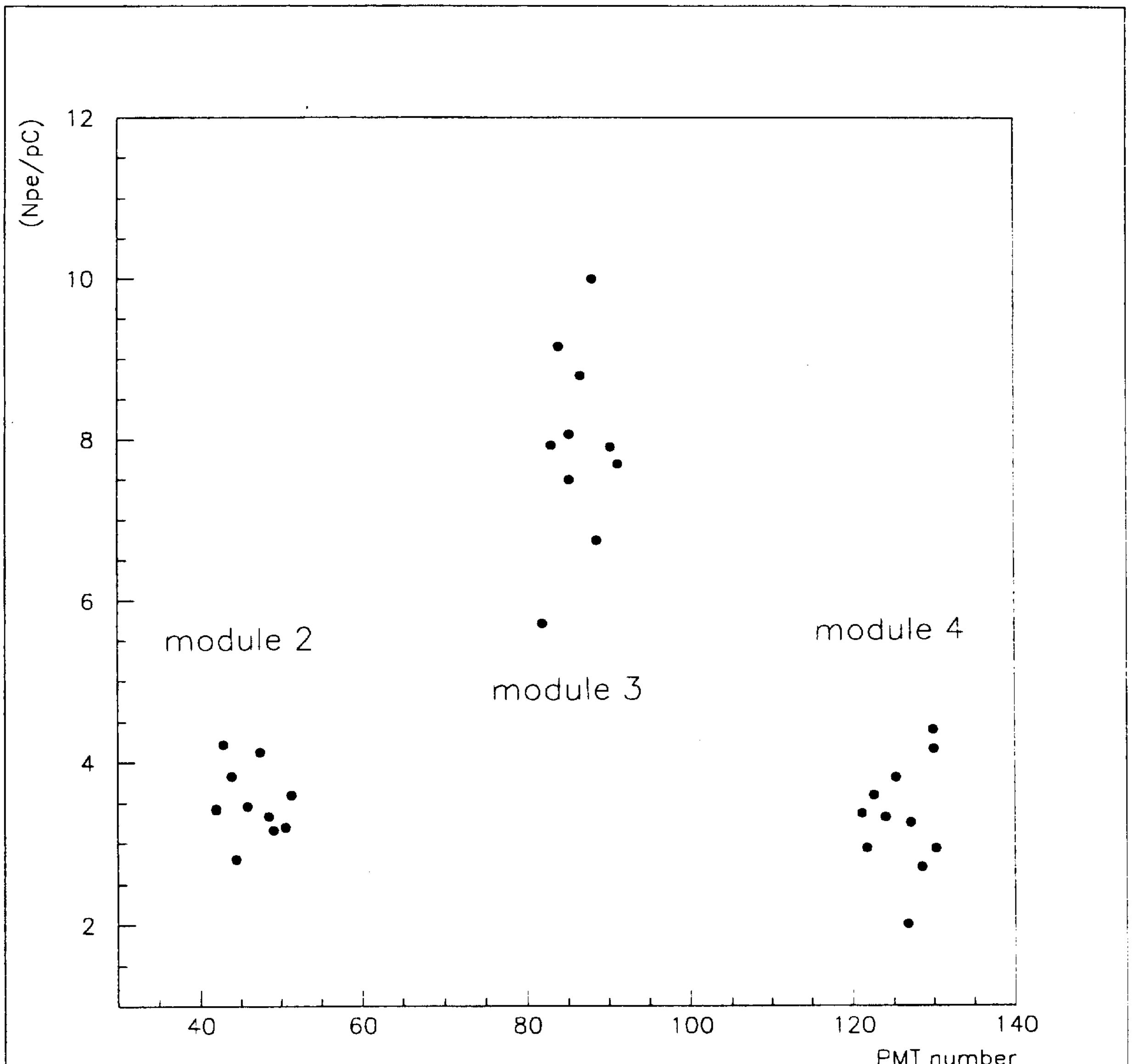

(Npe/pC)
12
10
8
6
4
2
module 2
module 3
module 4
40
60
80
100
120
140
PMT number

figure 18